

Analysis of Failure Modes in Fiber Reinforced Concrete Using X-ray Tomography and Digital Volume Correlation [†]

Mathias Flansbjer ^{1,*}, Natalie Williams Portal ¹, Stephen Hall ² and Jonas Engqvist ²

¹ Mechanics Research, RISE Research Institutes of Sweden, 50115 Borås, Sweden; Natalie.williamsportal@ri.se

² Solid Mechanics, Lund University, 221 00 Lund, Sweden; stephen.hall@solid.lth.se (S.H.); jonas.engqvist@solid.lth.se (J.E.)

* Correspondence: mathias.flansbjer@ri.se; Tel.: +46-10-516-5225

[†] Presented at the 18th International Conference on Experimental Mechanics, Brussels, Belgium, 1–5 July 2018.

Published: 19 May 2018

Abstract: Pull-out mechanisms for different common steel fibers were investigated using adapted pull-out tests performed in-situ in an X-ray micro tomograph (μ XRT). High-resolution volume images from the μ XRT scans enable clear visualization of aggregates, pores, the fiber and the fiber-matrix interface. Furthermore, the natural density speckle pattern from aggregate distribution and pores was found suitable for Digital Volume Correlation (DVC) analysis. From the DVC results it was possible to visualize and quantify the strain distribution in the matrix around the fiber at the different load levels up to final failure, being marked by either pull-out or fiber rupture. This study demonstrates that strain measurements within the concrete matrix can be obtained successfully using μ XRT imaging and DVC analysis, which leads to an increased understanding of the interaction mechanisms in fibre reinforced concrete under mechanical loading.

Keywords: fiber reinforced concrete; pull-out behavior; X-ray Computed Tomography; Digital Volume Correlation

1. Introduction

Fiber pull-out is generally considered to be the dominating failure mechanism in fiber reinforced concrete (FRC) to mitigate brittle failure. Accordingly, pull-out tests are typically performed on FRC to characterize the fiber-matrix behavior and estimate average tensile stresses near a crack opening. However, little direct insight can be gained on the actual mechanisms of the pull-out from such test, whereas, a deeper understanding of the underlying interaction mechanisms between discrete fibers and the surrounding concrete matrix could clearly lead to optimized FRC. Such deeper understanding could be gained through the addition of non-destructive techniques to pull-out tests to enable the visualization and quantification of the mechanical interaction between the fibers and the concrete matrix.

X-ray micro-tomography (μ XRT) is a non-destructive 3D imaging technique that has in recent years become a useful tool in engineering and material science to characterize the internal structures and mechanisms of a wide range of materials [1,2]. μ XRT has most commonly been applied on unloaded material samples, but with in-situ devices it is possible to run mechanical tests within a tomograph thus enabling scanning during loading of specimens [3]. Coupling of μ XRT with Digital Volume Correlation (DVC) has been applied to analyze the interior structural evolution of an array of materials, e.g., concrete [4], bone [5], wood [6], rock [7] and granular materials [8]. DVC can

essentially be considered as an extension of Digital Image Correlation (DIC) applied to tomographic image volumes to calculate full 3D vector displacements, from which tensor strain fields can be derived.

This paper presents the development of a method enabling the visualization and quantitative analysis of the fiber-matrix interaction on a meso-mechanical level in FRC samples. Reference tests are first described that provided characterization of the pull-out behavior of a steel fiber centrally cast in small cylindrical concrete specimens. These tests were also used to determine load levels at which μ XRT imaging was performed during pull-out tests in-situ in an X-ray tomograph. The pull-out test rig, tailored to the constraints of the μ XRT equipment and mechanical loading configuration, is described. Results from the tests and analysis, including using DVC, are presented and discussed for one fiber type in terms of the mechanical processes occurring in and around the fiber.

2. Materials and Methods

2.1. Selected Materials and Test Specimens

Cylindrical concrete specimens ($h = 50$ mm, $\varnothing = 43$ mm) each containing a singular steel fiber partly cast perpendicular and centric to the concrete surface (Figure 1a) were specifically prepared to accommodate a test setup having the possibility to apply a pull-out load while being placed in a tomograph. A high performance concrete mix developed for use in fiber-based reinforced concrete composites was used. This concrete mixture includes a CEM II/A-V 52.5 N Portland-fly ash cement, additional fly ash, chemical admixtures and a maximum aggregate size of 4 mm. The concrete was measured to have a compressive strength of 70 MPa and a tensile strength of 3.2 MPa at 28 days.

Six different steel fiber alternatives were selected for investigation, as illustrated in Figure 1b. These fibers have varying anchorage characteristics such as hooked-ends, hooked and flattened ends and wavy structure. A summary of general material and mechanical properties for the selected fibers is provided in Table 1. The embedded length, L_e , was set to 30 mm for all specimens. The scope of this paper is limited to Dramix 3D.

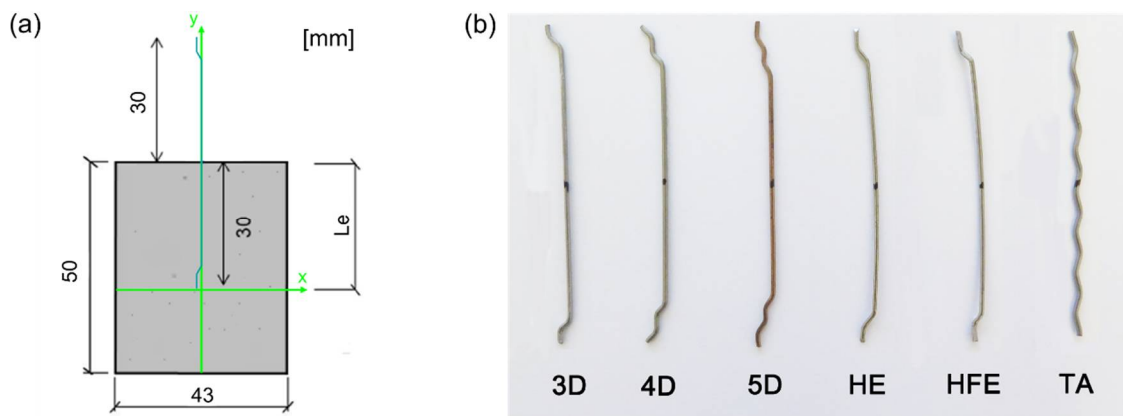


Figure 1. (a) Specimen geometry and (b) investigated fibers.

Table 1. Material properties for selected steel fiber alternatives.

ID	Product	Producer	Description of Fibre End	Length [mm]	Diameter [mm]	Tensile Strength [MPa]
3D	Dramix 3D 65/60	Bekaert	Hooked	60	0.9	1000
4D	Dramix 4D 65/60	Bekaert	Hooked	60	0.9	1500
5D	Dramix 5D 65/60	Bekaert	Hooked	60	0.9	2300
HE	HE 90/60	Arcelor Mittal	Hooked	60	0.9	1200
HFE	HFE 90/60	Arcelor Mittal	Flattened	60	0.9	1200
TA	Tabix+ 1/60	Arcelor Mittal	Wavy	60	1.0	1500

2.2. Reference Pull-Out Tests

A single-sided pull-out test was developed within the project, based on knowledge gathered from other studies (e.g., [9]), to simulate a stress-state present at a crack opening. This method makes it possible to characterize the behavior of individual fibers when pulled-out of the concrete matrix in terms of a load versus displacement relationship. Pull-out tests were firstly conducted without μ XRT according to Figure 2a to characterize the load-displacement relationship for the different FRC specimens. Based on the outcome of the results of these tests, the final test schedule and load levels for the pull-out tests with μ XRT were established. For example, suitable load levels for specimens with Dramix 3D fibers are indicated on the load-displacement curve in Figure 2b. Load levels prior to the peak load are relevant to be able to capture the initial debonding of the fiber and transition from mechanical adhesion to frictional bond. At load levels approaching the peak load, it is hypothesized that the plastic deformation of the fiber can likely be observed. In the case of pull-out failure, it could also be relevant to capture the extent of plastic deformation and pull-out of the fiber within the post-peak region.

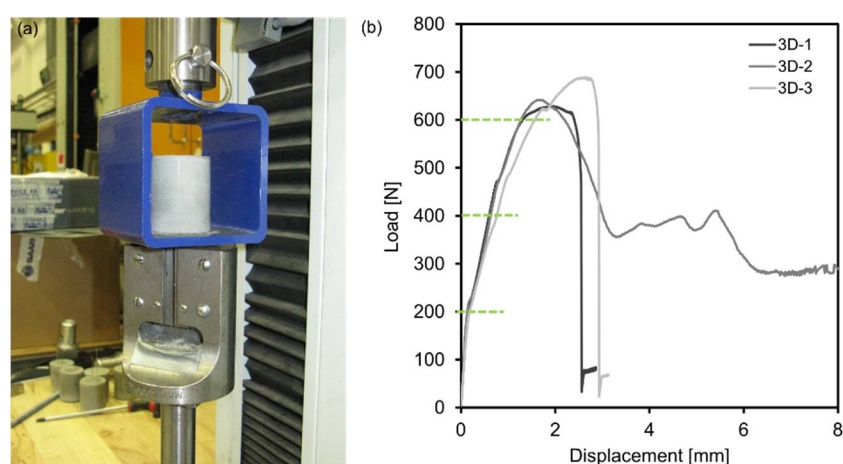


Figure 2. (a) Overview of reference pull-out test setup and (b) load-displacement curve for 3D specimens with indicated load levels for μ XRT.

2.3. Pull-Out Tests with μ XRT

The in-situ pull-out tests were performed in the Zeiss XRM520 at the 4D Imaging Lab at Lund University. A test specimen affixed to the loading device and a schematic of the test setup are shown in Figure 3. Each concrete specimen was mounted on the top of the device, above the piston and supported around its outer edge by a PMMA tube. The fibers protruding from each specimen were glued with HBM X60 into a threaded end anchorage that was screwed onto the piston of the test rig. The pull-out load was applied by controlled downward displacement of this piston.

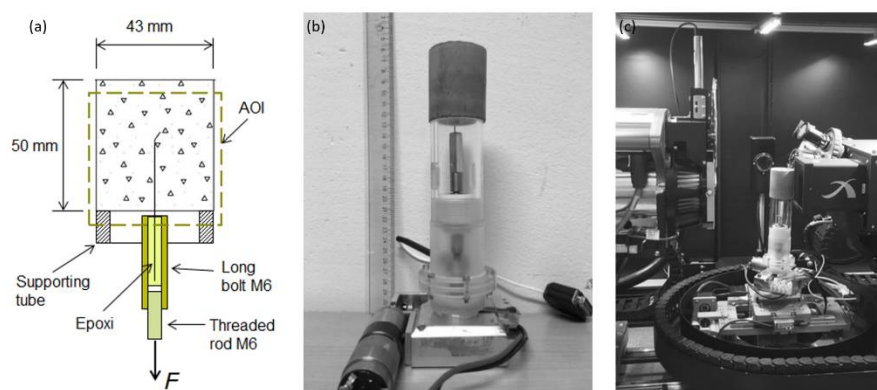


Figure 3. (a) Illustration of pull-out test setup up (cross section); (b) specimen affixed to loading device with long bolt and (c) overview of the μ XRT test set-up.

The μ XRT acquisitions involved 1601 radiographic projections over 360° with a 2 s exposure time using a source voltage of 160 kV and power of 10 W plus the He3-filter (as provided by the manufacturer) to reduce beam hardening artefacts. A $0.4\times$ objective was used and the camera binning was set to 2×2 giving images of 1024×1024 px. The voxels in the final reconstructed volumes were cubic with side lengths of 53 or 55 μm (depending on the test).

For each in-situ test, an initial scan was taken of the specimen prior to loading, which provided the undeformed reference image for the subsequent DVC-analyses. Thereafter, each specimen was loaded stepwise to the prescribed load levels at which new scans were made. One complete scan of the specimen took about 1 h at each load level, which amounts to approximately one day to execute a full test.

2.5. Processing with DVC

The StrainMaster software from LaVision was used for the DVC. The imported volume image is discretized into smaller sub-volumes containing unique grey-scale pattern. The software then correlates the pattern from the reference image to the deformed images and calculates the displacement within each sub-volume. This results in a full 3D vector field representing the specimen displacement, from which tensor strain fields are derived. In this study, the sub-volume size was set to $32 \times 32 \times 32$ voxels and the sub-volume overlap to 75%. This is approximately equivalent to a sub-volume size of $1.7 \times 1.7 \times 1.7$ mm and a resultant grid resolution of $0.4 \times 0.4 \times 0.4$ mm.

The region outside the specimen and the steel fiber itself was excluded from the DVC analysis using an algorithmic masking. It is to say that lower and upper threshold limits of the grey-scales in the volume image were specified. Furthermore, for a sub volume to be used, the requirement of minimum number of valid voxels inside the sub volume was set to 90%. This provides more reliable results at the edge of the analyzed volume and, most importantly in this case, at the fiber-matrix interface.

3. Results

From the high-resolution μ XRT images it was possible to have clear visualization of aggregates, pores, the fibers and the fiber-matrix interfaces. Furthermore, the natural grey-scale speckle in the images due to the chosen aggregate distribution and pores was found to be suitable for DVC analysis.

Two specimens with Dramix 3D fibers were tested, denoted as 3D-4 and 3D-5. Each specimen was imaged by μ XRT at different load levels selected based on the load-displacement relations obtained in the reference pull-out tests. Images were acquired before and after peak load, as depicted in Figure 4. Since the displacement was kept constant during the time of scanning, some relaxation in load could be observed at some of the scanning occasions.

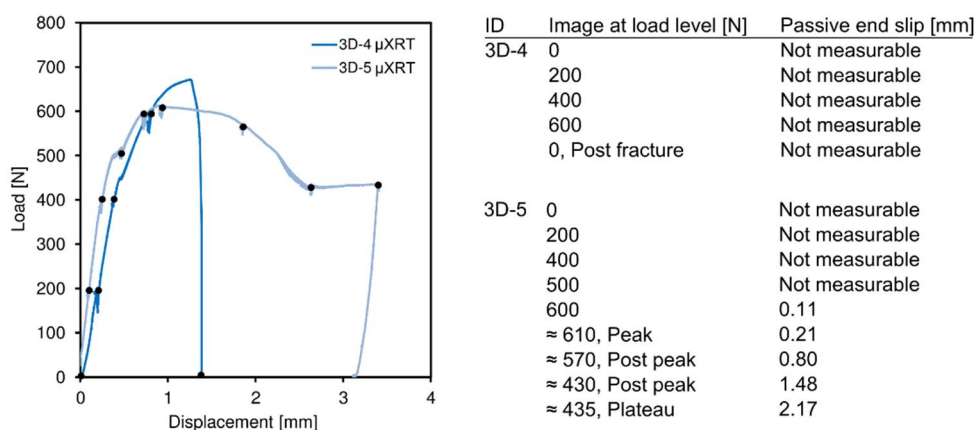


Figure 4. Load-displacement curves for 3D-4 and 3D-5 with indicated load levels applied for μ XRT scanning and measured passive end slip.

The reconstruction of μ XRT images provides a great deal of information related to both the geometry of the test specimen and the internal mechanisms taking place during loading. It is possible to distinguish the fibers final position in the specimen as well as the aggregate and pore distribution at the fiber interface. Moreover, the slipping or rupturing of the fiber within the so-called fiber canal can also be visualized. Furthermore, the DVC analysis of the time-series of volume images enabled the quantification of strains in the sample as well as the visualization of process details that were not visible simply from the tomography images. Figure 5 presents how the hooked steel fiber in specimen 3D-5 deformed and slipped inside the canal at three different stages of the loading. The passive end slip was evaluated as the pixel distance (i.e., 1 px = 53 μ m) between the fiber end and the bottom of the fiber canal. It was concluded that the fiber end started to slip around 500 N for specimen 3D-5, while no end slip was observed before fiber rupture occurred at 670 N for specimen 3D-4.

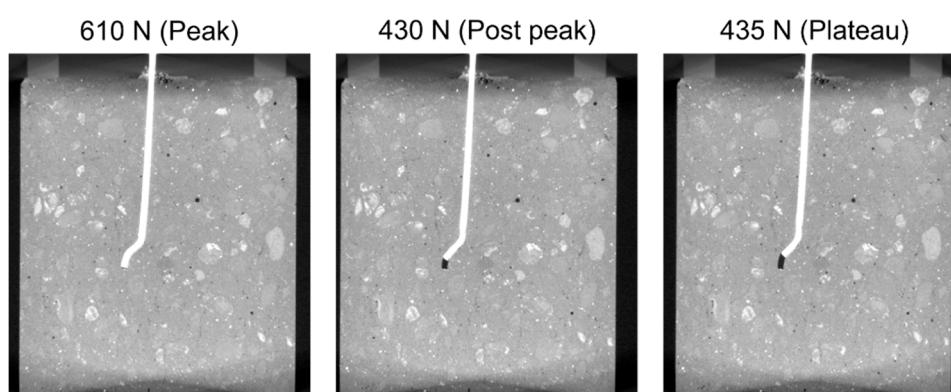


Figure 5. μ XRT images at selected load levels for specimen 3D-5.

From the DVC analysis, it is possible to observe a change in the load transfer mechanism between the steel fibre and the concrete matrix. During the initial linear part of the load-displacement curve, elevated shear strains can be observed along and around the fibre, which according to theory can be due to adhesion and frictional bond, as exemplified in Figure 6 at a load level of 400 N. When the fibre starts to slip around 500 N, the end-hook acts as a mechanical interlock since it is forced to deform to be able to slip. The load transfer between the fibre and matrix becomes thereby localised at the hook, resulting in high local compressive strains (minimum principal strains) and shear strains at 500 and 600 N. At 435 N, it can be observed that mechanical locking is still active for larger end slip values. This mechanical locking effect is presumed to be active until the fibre hook has deformed plastically and becomes straight and slips in the main vertical canal. The strains that are surrounding the bottom of the fibre canal are thought to be caused by the contraction of the void left by the fibre.

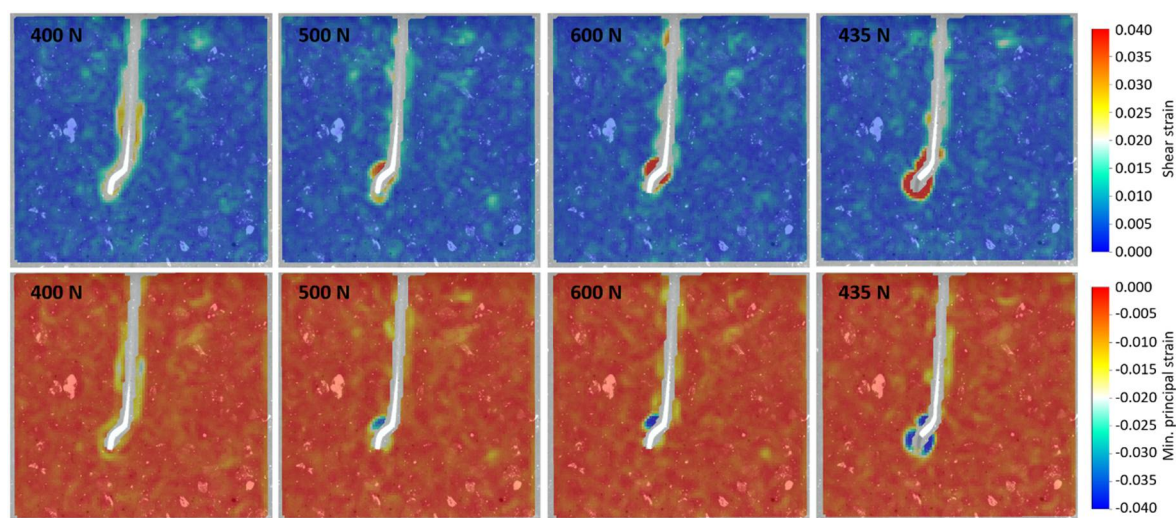


Figure 6. Shear and principle strain from DVC analysis of specimen 3D-5 at 400, 500, 600 and 435 N.

4. Conclusions

Pull-out mechanisms for steel fibers were investigated using adapted pull-out tests performed in-situ in a μ XRT. High-resolution volume images from the μ XRT scans enable clear visualization of aggregates, pores, the fiber and the fiber-matrix interface. Furthermore, the natural density speckle pattern from aggregate distribution and pores was found suitable for DVC analysis. From the DVC analysis, it was possible to visualize and quantify the strain distribution in the matrix around the fiber at the different load levels up to final failure, which was marked by either pull-out or fiber rupture. The load transfer mechanism was initially dominated by shear along the fiber. As the load increased, slip occurred in the end-hook region and mechanical locking became the governing mechanism. This study demonstrates that strain measurements within the concrete matrix can be obtained successfully using μ XRT imaging and DVC analysis, which leads to an increased understanding of the interaction mechanisms between the fiber and the concrete matrix.

Author Contributions: M.F. and N.W.P. designed and analyzed pull-out test experiments; S.H. and J.E. performed pull-out tests with μ XRT and reconstruction of μ XRT scanning images; M.F. performed DVC analysis; N.W.P., M.F. and S.H. wrote the paper.

Acknowledgments: The presented research was made possible with the support of Åforsk (ref No. 15-520).

Conflicts of Interest: The authors declare no conflict of interest.

References

1. Maire, E.; Withers, P.J. Quantitative X-ray tomography. *Int. Mater. Rev.* **2014**, *59*, 1–43, doi:10.1179/1743280413Y.0000000023.
2. Landis, E.N.; Keane, D.T. X-ray microtomography. *Mater. Charact.* **2010**, *61*, 1305–1316, doi:10.1016/j.matchar.2010.09.012.
3. Buffiere, J.Y.; Maire, E.; Adrien, J.; Masse, J.P.; Boller, E. In Situ Experiments with X ray Tomography: An Attractive Tool for Experimental Mechanics. *Exp. Mech.* **2010**, *50*, 289–305, doi:10.1007/s11340-010-9333-7.
4. Yang, Z.J.; Ren, W.Y.; Mostafavi, M.A.; McDonald, S.A.; Marrow, T.J. Characterisation of 3D fracture evolution in concrete using in-situ X-ray computed tomography testing and digital volume correlation. In Proceedings of the VIII International Conference on Fracture Mechanics of Concrete and Concrete Structures, Toledo, Spain, 10–14 March 2013.
5. Gillard, F.; Boardman, R.; Mavrogordato, M.; Hollis, D.; Sinclair, I.; Pierron, F.; Browne, M. The application of digital volume correlation (DVC) to study the microstructural behaviour of trabecular bone during compression. *J. Mech. Behav. Biomed. Mater.* **2014**, *29*, 480–499.
6. Forsberg, F.; Sjö Dahl, M.; Mooser, R.; Hack, E.; Wyss, P. Full Three-Dimensional Strain Measurements on Wood Exposed to Three-Point Bending: Analysis by Use of Digital Volume Correlation Applied to Synchrotron Radiation Micro-Computed Tomography Image Data. *Strain* **2010**, *46*, 47–60, doi:10.1111/j.1475-1305.2009.00687.x.
7. Mao, L.; Zuo, J.; Yuan, Z.; Chiang, F.P. Full-field mapping of internal strain distribution in red sandstone specimen under compression using digital volumetric speckle photography and X-ray computed tomography. *J. Rock Mech. Geotech. Eng.* **2015**, *7*, 136–146.
8. Hall, S.A.; Bornert, M.; Desrues, J.; Pannier, Y.; Lenoir, N.; Viggiani, G.; Bésuelle, P. Discrete and continuum analysis of localised deformation in sand using X-ray μ CT and volumetric digital image correlation. *Géotechnique* **2010**, *60*, 315–322.
9. Breitenbücher, R.; Meschke, G.; Song, F.; Zhan, Y. Experimental, analytical and numerical analysis of the pullout behaviour of steel fibres considering different fibre types, inclinations and concrete strengths. *Struct. Concr.* **2014**, *15*, 126–135.

